Jurnal Tribologi 23 (2019) 76-89

MYTRIBOS Malaysian Tribology Society

Jurnal Tribologi

Website : jurnaltribologi.mytribos.org e-issn: 2289-7232

Optimization of wear parameters of magnesium metal-metal composite using Taguchi and GA technique

Sathish, S. [1,*], Anandakrishnan, V. [1], Sankaranarayanan, S. [2], Gupta, M. [2]

[1] National Institute of Technology Tiruchirappalli, Tanjore Main Road, National Highway 67, Near BHEL Trichy, Tiruchirappalli, Tamil Nadu 620015, INDIA.
[2] National University of Singapore, 9 Engineering Drive 1, Singapore 117576, SINGAPORE.
*Corresponding author: sadish.kss@gmail.com

KEYWORDS

Magnesium
Metal-metal composite
Dry sliding
Wear mechanism
Wear debris

ABSTRACT

A novel magnesium-aluminium-titanium composite was successfully fabricated through disintegrated melt deposition technique and its tribology was analysed. The metallurgical analyses display the distribution of added metallic reinforcement on the developed metal-metal composite. By following ASTM standard, the wear test was completed on pin-on-disc apparatus, wear and coefficient of friction were recorded. Taguchi's approach and genetic algorithm technique were used to analyze the parametric influence on the tribology of the synthesized metal-metal composite and to identify the optimal solution. (1) The Taguchi analysis recognized the optimal parameter as 9.81 N, 3 m/s and 2000 m (2) The Genetic algorithm technique recognized the optimal parameter as 9.81 N, 3 m/s and 1999.9 m (3) The developed regression model showed closer value with experimental results (4) The governing wear mechanisms were identified as abrasion, adhesion, softening, melting, and delamination.

1.0 INTRODUCTION

Composite technology provides the opportunity to tailor-made materials according to the requirements of end applications. Generally, metal matrix, ceramic matrix and polymer matrix composites are produced through the addition of reinforcements in the form of borides, oxides and carbides. Metal-metal composites represent composites which contain metals as reinforcement. As metals are comparative ductile and deformable when compared to ceramics, the particle damage mechanisms are minimized leading to a good combination of strength and

Received 13 August 2019; received in revised form 25 September 2019; accepted 2 November 2019.
To cite this article: Sathish et al. (2019). Optimization of wear parameters of Magnesium metal-metal composite using Taguchi and GA technique. Jurnal Tribologi 23, pp.76-89.

ductility (Krishna et al., 2017). Matrix material selection for composites is primarily based on its end application. However, additional factors such as environmental compatibility, energy efficiency are also tagged to material selection. One such metallic material that suits the above needs is magnesium due to its low density and high specific strength (Aydin and Findik, 2010). Such attributes are particularly desirable for weight critical applications such as in the transportation and defense sectors (Niranjan et al., 2018). Numerous research attempts were made to utilize composite technology to improve the properties of magnesium. Magnesium based metal-metal composites were fabricated containing Ti6Al4V powder as reinforcement, and a uniform distribution of reinforcement was reported (Braszczyńska-Malik and Przełożyńska, 2014). Considerable improvement in properties of a magnesium composite containing 10 weight percentage titanium carbide synthesized using self-propagating high temperature technique was reported (Mehra et al., 2018). Magnesium composite with 10 volume percentage of Ti2AlC was produced through stir casting route trailed by hot extrusion and improved tensile strength, compressive strength and the thermal conductivity were reported by Yu et al. (Yu et al., 2018). Wang et al. synthesized in-situ magnesium composite with graphene reinforcement using casting route and reported improved strength and ductility (Wang et al., 2018). Hou et al. synthesized magnesium composites with carbon nanotubes as reinforcement through powder metallurgy route and observed a 28 percentage rise in tensile strength (Hou et al., 2018). Castro et al. synthesized magnesium composite using machined magnesium chip and alumina reinforcement by cold consolidation technique and observed improved hardness and creep resistance (Castro et al., 2019). Hassan et al. synthesized Mg-TiO_2 nanocomposites using powder metallurgy coupled with hot extrusion and reported improved ductility while the strength remained unaffected (Hassan et al., 2018). Watanabe et al. synthesized biodegradable magnesium composite containing 0.5 mass percentage of calcium and 10 volume percentage of β-tricalcium phosphate and reported an improved tensile strength (Watanabe et al., 2018). Rashad et al. synthesized magnesium composite with 10 % titanium and 1 % aluminium using semi powder metallurgy route and hot extrusion and reported improved tensile strength (Rashad et al., 2015). Sankaranarayanan et al. synthesized Mg-Al/Ti composites using disintegrated melt deposition technique and reported an improvement in strength and ductility (Sankaranarayanan et al., 2011). Habibi et al. synthesized Mg-Al/ B4C composites using microwave assisted sintering technique coupled with hot extrusion and reported an improvement in strength (Habibi, et al., 2013). Kaviti et al. investigated the tribological behaviour of Mg/BN composites and observed a lower wear rate at 0.5% of boron nitride (Kaviti et al., 2018). Turan et al. investigated the tribological response of magnesium composite with fullerene reported higher wear resistant at 0.5 weight percentage addition of fullerene (Turan et al., 2018a). Tribological behaviour of carbon nanotubes reinforced magnesium composite was investigated by Zhang et al. and they reported a reduction in wear rate due to the presence of carbon nanotubes (Zhang et al., 2018). Mehra et al. investigated the tribological behaviour of Mg/TiC composites and observed the wear rate decreased with an increase in TiC content (Mehra et al., 2018). From the outlook of earlier research findings, the present work is focused on the synthesis of magnesium metal-metal composite through disintegrated melt deposition route containing 3 and 5.6 weight percentage of aluminium (alloying element similar to AZ 31 alloy) and titanium (immiscible with Mg and serves as reinforcement) elements, respectively. Further to investigate the tribological behaviour of the magnesium metal-metal composite, Taguchi's technique and genetic algorithm technique were used to analyze the wear test results obtained from standard pin-on-disc equipment.

2.0 EXPERIMENTAL PROCEDURE

Magnesium based metal-metal composite was synthesized with the addition of 3 wt. % aluminium and 5.6 weight percent titanium. Pure magnesium with measured quantities of elements was melted using an electrical resistance furnace in an argon atmosphere to a temperature of 750°C. After the realization of molten state, the melt was stirred at 460 rpm for 5 minutes with a Zirtex 25 coated steel stirrer. Subsequently, the stirred melt was allowed to flow through a 10-mm orifice, disintegrated by two argon jets and deposited as a cylindrical ingot of 40mm diameter. Subsequently, the ingot was hot extruded at an extrusion ratio of 20.25:1, to obtain cylindrical rods of 8mm diameter (Sankaranarayanan et al., 2011). Samples obtained by segmenting the extruded rod using the wire electric discharge machine were polished and subjected to X-ray diffraction and scanning electron microscopy and energy dispersive spectroscopic analysis. Similarly, samples of 8mm diameter and 20mm height were also segmented from the hot extruded metal-metal composite and their ends were polished for wear analysis. Figure 1 shows the picture of pin-on-disc experimental setup along with the schematic diagram. As per ASTM-G99 standard, dry sliding wear tests were performed under a varied combination of parameters namely sliding velocity (1, 2 and 3 m/s) and applied load (9.81, 19.62 and 29.43 N) over 2000 m sliding distance (Baskaran et al., 2014; Saravanan et al., 2018; Sathish et al., 2019; Selvam et al., 2014). From the wear experiments, the specific wear and coefficient of friction were obtained and the same are shown in Table 1.

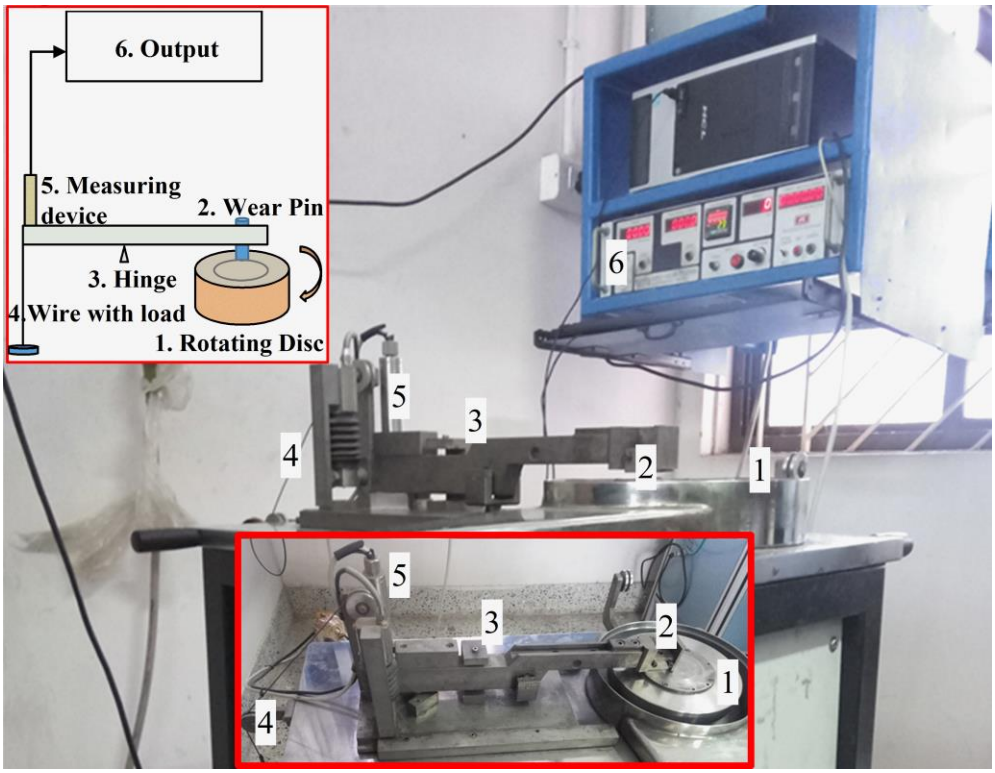

Figure 1: Pin-on-disc experimental setup.

Table 1: Experimental design with specific wear and coefficient of friction.

S. No	Load, N	Sliding Velocity, m/s	Sliding distance, m	Specific wear, micron	COF
1	9.81	1	500	0.17384	0.05301
2	9.81	1	1000	0.17025	0.04893
3	9.81	1	1500	0.16547	0.04281
4	9.81	1	2000	0.19250	0.04179
5	9.81	2	500	0.25338	0.11060
6	9.81	2	1000	0.19775	0.11083
7	9.81	2	1500	0.17928	0.10887
8	9.81	2	2000	0.16898	0.10005
9	9.81	3	500	0.18686	0.12538
10	9.81	3	1000	0.14763	0.12538
11	9.81	3	1500	0.13296	0.11621
12	9.81	3	2000	0.12433	0.12029
13	19.62	1	500	0.34418	0.12718
14	19.62	1	1000	0.31155	0.12966
15	19.62	1	1500	0.29946	0.12875
16	19.62	1	2000	0.29300	0.11988
17	19.62	2	500	0.22374	0.17409
18	19.62	2	1000	0.22614	0.17227
19	19.62	2	1500	0.22934	0.16884
20	19.62	2	2000	0.22912	0.15957
21	19.62	3	500	0.20362	0.15644
22	19.62	3	1000	0.17107	0.15424
23	19.62	3	1500	0.16010	0.15322
24	19.62	3	2000	0.15600	0.15373
25	29.43	1	500	0.47814	0.22562
26	29.43	1	1000	0.42677	0.21101
27	29.43	1	1500	0.41010	0.21543
28	29.43	1	2000	0.37300	0.22188
29	29.43	2	500	0.32442	0.22222
30	29.43	2	1000	0.29651	0.21441
31	29.43	2	1500	0.29045	0.20863
32	29.43	2	2000	0.28550	0.20829
33	29.43	3	500	0.20644	0.21509
34	29.43	3	1000	0.18885	0.20217
35	29.43	3	1500	0.17997	0.20591
36	29.43	3	2000	0.17500	0.19300

3.0 REGRESSION MODELLING

The regression model for specific wear and coefficient of friction was generated (Zain et al., 2011) with the parameters load (L), sliding velocity (V) and sliding distance (D) and it is expressed with the relation as shown in Eq. (1).

$$Response = c\ L^p V^q D^r \varepsilon \quad (1)$$

Where, c, p, q and r are the model parameters, and ε is the experimental error. With the above, a second order polynomial equation was generated as shown in Eq. (2) as reported by Zain et al. (Zain et al., 2011).

$$y = b_0 + b_1 \times L + b_2 \times V + b_3 \times D + b_{12} \times L \times V + b_{13} \times L \times D + b_{23} \times V \times D \quad (2)$$

4.0 RESULTS AND DISCUSSION

4.1 Metallurgical Analysis

The X-Ray diffraction analysis of the (Mg-3Al)/5.6Ti metal-metal composite exhibited the peaks as shown in Fig. 2. It shows the peaks of magnesium, titanium and the intermetallic phase ($Mg_{17}Al_{12}$) with the plane indices of (011), (011), and (033) respectively. Fig. 3 shows the microstructure of (Mg-3Al)/5.6Ti metal-metal composite with the existence of titanium phase as it is insoluble in magnesium. As the aluminium is soluble, it results in the formation of $Mg_{17}Al_{12}$ and the same is not observed in the microscopic analysis as the quantity is found to be less (Sankaranarayanan et al., 2011). Further, the presence of added elements is also confirmed through the energy dispersive spectroscopy (EDS) analysis and the elemental map obtained from the analysis is shown in the merged form in Fig. 4 and this confirms the existence of added magnesium (light yellow colour), titanium (red colour) and aluminium (green colour) in the (Mg-3Al)/5.6Ti metal-metal composite.

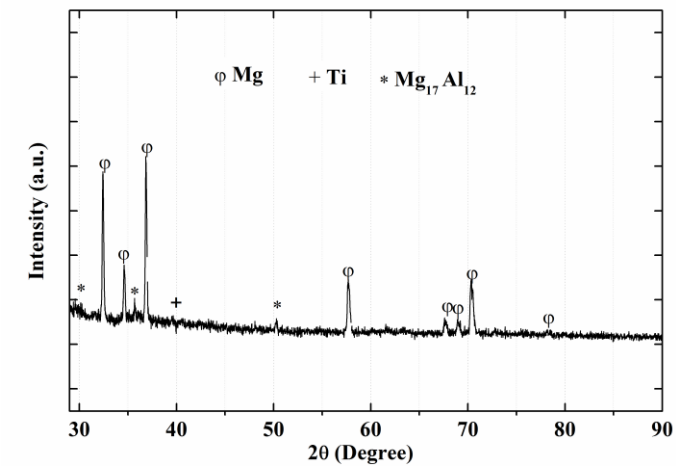

Figure 2: X-Ray diffraction of (Mg-3Al)/5.6Ti metal-metal composite.

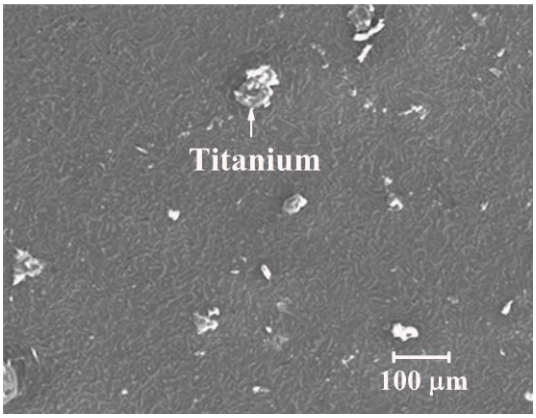

Figure 3: Microstructure of (Mg-3Al)/5.6Ti metal-metal composite.

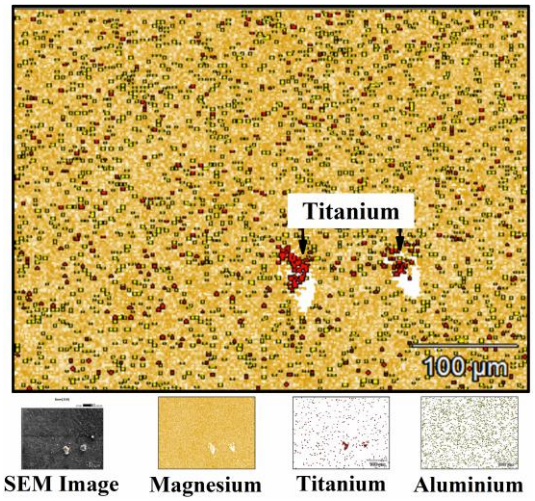

Figure 4: Elemental map of (Mg-3Al)/5.6Ti metal-metal composite.

4.2 Tribological Analysis by Taguchi's Approach

From the dry sliding wear tests, the response specific wear and coefficient of friction are obtained as shown in Table 1, and the analysis was performed using Taguchi's approach. "Lower the better" quality characteristic was used in the present analysis as the objective was to obtain minimum specific wear and minimum coefficient of friction (Sarkar et al., 2018; Maleque et al., 2018). The analysis results in the main effect plot shown in Fig. 5 gives the optimum parameters to obtain the minimum specific wear (Fig. 5a) and minimum coefficient of friction (Fig. 5b). The best parameters to obtain the minimum specific wear is 9.81 N of load, 3 m/s of sliding velocity and 2000 m of sliding distance and the best parameters to obtain the minimum coefficient of friction is 9.81 N of load, 1 m/s of sliding velocity and 2000 m of sliding distance.

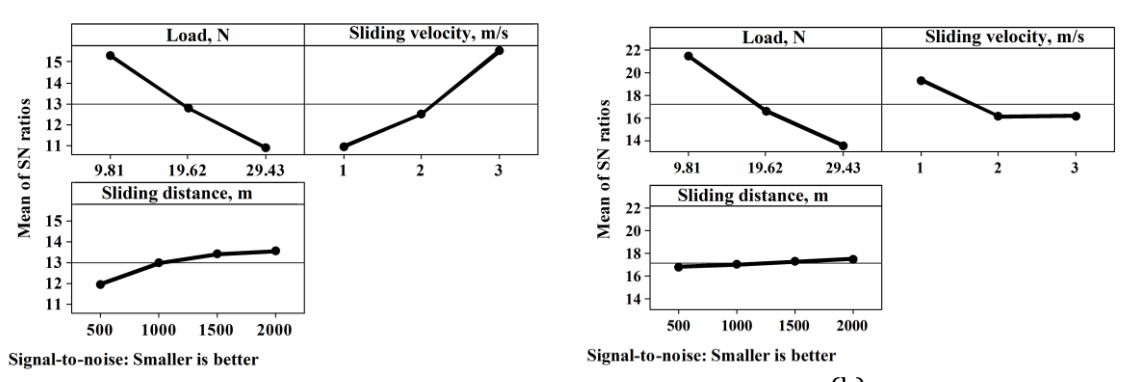

Figure 5: Main effect plot: (a) Specific wear, and (b) coefficient of friction.

The analysis of variance for the given response shows the significant parameters, which has a more contributing effect on the response specific wear and coefficient of friction (Monikandan et al., 2018). Table 2 shows the analysis of variance for specific wear with a higher probability percentage of 39.72 for sliding velocity, followed by load and for the interaction of load and sliding velocity with the probability percentage of 36.55 and 17.41 respectively. Further, it also shows that both the load and sliding velocity has its significant contributions by individual and also combined together in the wear behaviour of the produced metal-metal composite. Table 3 shows the analysis of variance for the coefficient of friction with a higher probability percentage of 82.90 for load, followed by the interaction of load and sliding velocity and sliding velocity with the probability percentage of 8.71 and 7.51, respectively. The analysis for the both response shows the significance with load and sliding velocity.

Table 2: Analysis of variance for specific wear.

Parameters	**DF[a]**	**Seq SS[b]**	**Adj SS[c]**	**Adj MS[d]**	**F**	**P[e]**	**P%**
Load	2	0.099079	0.099079	0.04954	101.13	0.000	36.55
Sliding Velocity	2	0.107658	0.107658	0.053829	109.88	0.000	39.72
Sliding distance	3	0.010415	0.010415	0.003472	7.09	0.005	03.84
Load*Sliding Velocity	4	0.047202	0.047202	0.011801	24.09	0.000	17.41
Load*Sliding distance	6	0.000766	0.000766	0.000128	0.26	0.945	0.28
Sliding Velocity * Sliding distance	6	0.000073	0.000073	0.000012	0.02	1.000	0.03
Error	12	0.005879	0.005879	0.00049			2.17
Total	35	0.271072					

S = 0.0221331 R-Sq = 97.83% R-Sq(adj) = 93.67%

[a]Degrees of freedom, [b]Sequential sums of squares, [c]Adjusted sums of squares, [d]Adjusted mean squares, [e]Probability

Table 3: Analysis of variance for coefficient of friction.

Parameters	DF[a]	Seq SS[b]	Adj SS[c]	Adj MS[d]	F	P[e]	P%
Load	2	0.0863793	0.0863793	0.0431897	2175.86	0.000	82.90
Sliding Velocity	2	0.0078262	0.0078262	0.0039131	197.14	0.000	7.51
Sliding distance	3	0.0004873	0.0004873	0.0001624	8.18	0.003	0.47
Load*Sliding Velocity	4	0.0090708	0.0090708	0.0022677	114.25	0.000	8.71
Load*Sliding distance	6	0.0001418	0.0001418	0.0000236	1.19	0.374	0.14
Sliding Velocity * Sliding distance	6	0.0000507	0.0000507	0.0000084	0.43	0.848	0.05
Error	12	0.0002382	0.0002382	0.0000198			0.23
Total	35	0.1041942					

S = 0.00445527 R-Sq = 99.77% R-Sq(adj) = 99.33%

[a]Degrees of freedom, [b]Sequential sums of squares, [c]Adjusted sums of squares, [d]Adjusted mean squares, [e]Probability

A regression model was generated for specific wear and coefficient of friction with the regression coefficient of 95.37 and 96.09 percentage as shown in Eq. (3) and (4). With the generated model, the specific wear and coefficient of friction were predicted (shown in Table 4) in order to validate the model. The generated model showed the least error percentage of 6.71 and 7.63 for specific wear and coefficient of friction, respectively and is found to be more suitable.

$$\text{Specific Wear} = 0.0598767 + 0.0176678 \times \text{Load} + 0.0370729 \times \text{Sliding Velocity} - 0.00001859 \times \text{Sliding distance} - 0.00527185 \times \text{Load} \times \text{Sliding Velocity} - 0.000000459967 \times \text{Load} \times \text{Sliding distance} - 0.000000425889 \times \text{Sliding Velocity} \times \text{Sliding distance} \quad (3)$$

$$\text{Coefficient of friction} = -0.0835653 + 0.0107629 \times \text{Load} + 0.0607218 \times \text{Sliding Velocity} - 0.00000346951 \times \text{Sliding distance} - 0.00228388 \times \text{Load} \times \text{Sliding Velocity} - 0.0000000647597 \times \text{Load} \times \text{Sliding distance} - 0.000000892682 \times \text{Sliding Velocity} \times \text{Sliding distance} \quad (4)$$

Table 4: Predicted specific wear and coefficient of friction.

S. No	Specific wear, micron	COF	Error, %	Accuracy, %	Error, %	Accuracy, %
1	0.20679	0.05784	15.93	84.07	8.35	91.65
2	0.19503	0.05534	12.70	87.30	11.58	88.42
3	0.18326	0.05284	9.71	90.29	18.97	81.03
4	0.17150	0.05034	12.25	87.75	16.98	83.02
5	0.19193	0.09571	32.01	67.99	15.56	84.44
6	0.17996	0.09276	9.89	90.11	19.47	80.53
7	0.16798	0.08982	6.73	93.27	21.21	78.79
8	0.15600	0.08687	8.32	91.68	15.17	84.83
9	0.17708	0.13358	5.53	94.47	6.14	93.86
10	0.16489	0.13019	10.47	89.53	3.69	96.31
11	0.15270	0.12680	12.93	87.07	8.35	91.65
12	0.14051	0.12340	11.51	88.49	2.53	97.47
13	0.32614	0.14070	5.53	94.47	9.61	90.39
14	0.31212	0.13788	0.18	99.82	5.96	94.04

15	0.29810	0.13507	0.46	99.54	4.67	95.33
16	0.28408	0.13225	3.14	96.86	9.35	90.65
17	0.25956	0.15616	13.80	86.20	11.48	88.52
18	0.24533	0.15290	7.82	92.18	12.67	87.33
19	0.23110	0.14964	0.76	99.24	12.83	87.17
20	0.21686	0.14638	5.65	94.35	9.02	90.98
21	0.19299	0.17163	5.51	94.49	8.85	91.15
22	0.17854	0.16792	4.19	95.81	8.15	91.85
23	0.16410	0.16421	2.44	97.56	6.69	93.31
24	0.14965	0.16050	4.24	95.76	4.22	95.78
25	0.44549	0.22356	7.33	92.67	0.92	99.08
26	0.42921	0.22043	0.57	99.43	4.27	95.73
27	0.41293	0.21729	0.69	99.31	0.86	99.14
28	0.39666	0.21416	5.96	94.04	3.61	96.39
29	0.32720	0.21662	0.85	99.15	2.59	97.41
30	0.31071	0.21304	4.57	95.43	0.64	99.36
31	0.29422	0.20946	1.28	98.72	0.40	99.60
32	0.27773	0.20588	2.80	97.20	1.17	98.83
33	0.20890	0.20968	1.18	98.82	2.58	97.42
34	0.19220	0.20566	1.74	98.26	1.69	98.31
35	0.17550	0.20163	2.54	97.46	2.12	97.88
36	0.15880	0.19760	10.20	89.80	2.33	97.67
Average			6.71	93.29	7.63	92.37

4.3 Tribological Analysis by Genetic Algorithm

The genetic algorithm is a technique which helps to evolve the optimal solution through the generation of offspring with the available population set. It involves the sequence of steps namely population selection, reproduction, crossover and mutation with several iterations to obtain the optimal solution (Mukhopadhyay et al., 2016; Metawa et al., 2017). The present analysis focuses on the optimization of specific wear and coefficient of friction with minimization as the objective function. Based on the proposed regression model, Eq. (3) and Eq. (4) were considered as the fitness function with the boundaries as mentioned in Eq. (5-7). Table 5 shows the criteria selected for the optimization of a fitness function (Zain et al., 2011). With the above criteria and function, the optimization was performed in MATLAB R2018a software with an optimization tool box. From the analysis, the optimal solution for specific wear of 0.140506 microns was obtained at 124^{th} iteration with the parameter of 9.81 N of load, 3 m/s of sliding velocity and 2000 m of sliding distance. The optimal solution for the coefficient of friction of 0.050340 was obtained at 96^{th} iteration with the parameters of 9.81 N of load, 1 m/s of sliding velocity and 1999.999 m of sliding distance. From the fitness function plot (shown in Fig. 6), the best value of fitness was found as 0.140506 microns with the mean value of fitness as 0.140631 microns for specific wear from Fig. 6(a) and the best value of fitness is found as 0.0503407 with the mean value of fitness as 0.0567283 for the coefficient of friction from Fig. 6(b). Table 6 shows the comparison of results for the optimum combination of parameters with optimal solution and parameter combination is found to be same for both Taguchi's approach and genetic algorithm approach.

$$9.81 \leq L \leq 29.43 \quad (5)$$
$$1 \leq V \leq 3 \quad (6)$$
$$500 \leq D \leq 2000 \quad (7)$$

Table 5: Criteria for genetic algorithm.

Parameters	Function
Population type	Double vector
Population size	100
Scaling function	Rank
Selective function	Roulette wheel
Crossover function	Heuristic
Crossover rate	0.8
Mutation function	Adaptive

Table 6: Comparison of results.

Technique	Response	Optimum Parameters	Experimental value	Optimal Solution
Taguchi	Specific wear	9.81N, 3 m/s, 2000 m	0.12433	0.14051
	Coefficient of friction	9.81N, 1 m/s, 2000 m	0.04179	0.05034
Genetic Algorithm	Specific wear	9.81N, 3 m/s, 2000 m	0.12433	0.14050
	Coefficient of friction	9.81N, 1 m/s, 1999.99 m	-	0.05034

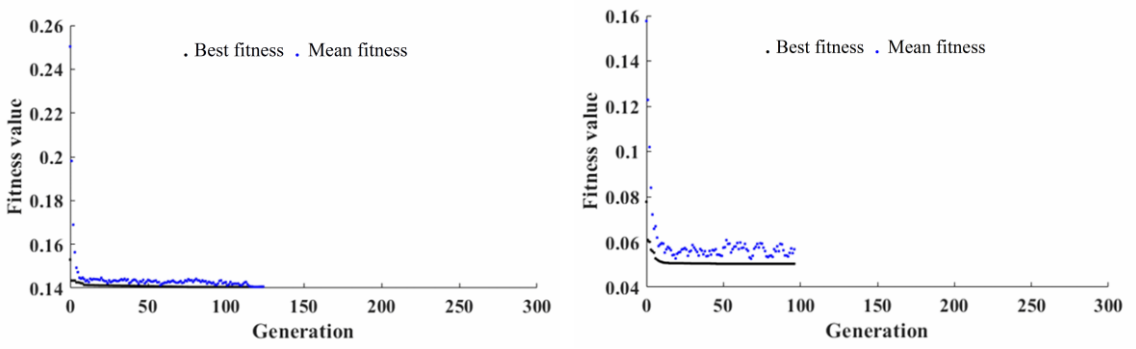

(a) (b)

Figure 6: Fitness plot: (a) Specific wear, and (b) coefficient of friction.

4.4 Wear Mechanisms

After the completion of the dry sliding wear test, the ends of sample pins were sectioned carefully and analyzed in scanning electron microscopy to explore the mechanisms involved in the dry sliding of magnesium composite. The worn surface of the wear pins related to the conditions of maximum wear (i.e., 29.43 N load, 1 m/s sliding velocity, 2000 m sliding distance) and minimum wear (i.e., 9.81 N load, 3 m/s sliding velocity, 2000 m sliding distance) are shown in Fig. 7(a) and Fig. 7(b) respectively. Fig. 7(a) shows the worn surface of wear pin for maximum wear condition with the existence of craters, scratches and fine debris, which displays the

mechanism of delamination and oxidation as reported elsewhere (Elleuch et al., 2006; Turan et al., 2018b; Zhang et al., 2018). The magnified view (inside Fig. 7(a)) displays the buildup material at the pin edge (Line shown in yellow colour) due to the accumulation of wiped material. A layer of a smooth glazed surface was also observed below the crater, which is due to the material softening followed by the action of sliding shows the existence of thermal softening of metal. The wear debris of maximum wear condition as shown in Fig. 8(a) shows the smooth layered large sheets and laminates which displays the mechanism of melting and softening. Fig. 7(b) shows the worn surface of wear pin for minimum wear condition with the existence of plastic deformed layers and the traces of smeared layer indicating the mechanism of adhesion consistent with the observation of other researchers (Elleuch et al., 2006; Zhang et al., 2018). Fig. 8(b) shows the wear debris relevant to the minimum wear condition with a long deformed layer of the lamina with series of furrows affirming adhesion mechanism and this attributes the extensive transfer of material because of plastic deformation.

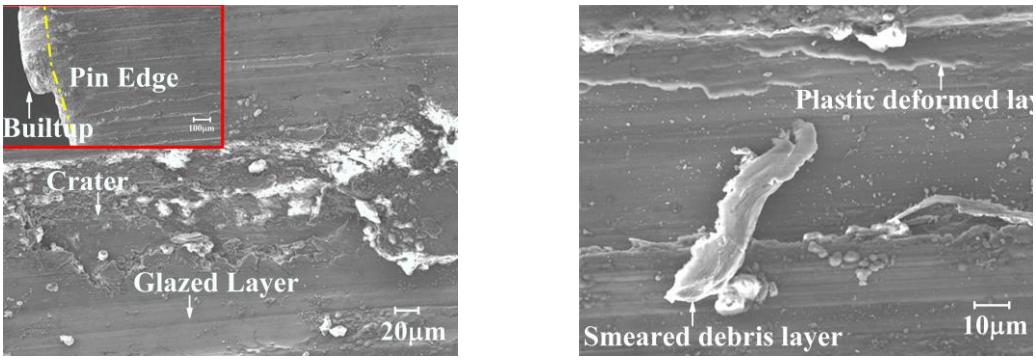

(a) (b)

Figure 7: Worn surface of pin at (a) Maximum wear, and (b) minimum wear.

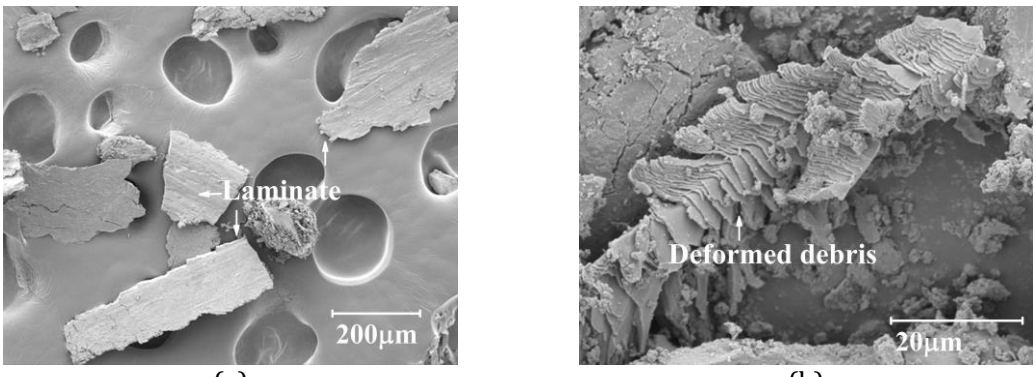

(a) (b)

Figure 8: Wear debris of (a) maximum wear, and (b) minimum wear.

4.5 Wear Map

Wear map obtained from the Taguchi approach is shown in Fig. 9 concerning the combination of load and sliding velocity. Wear map consists of three regions as mild wear region, medium wear region and severe wear region. Mild wear region represents specific wear less than 0.2 microns, medium wear region represents specific wear in the range of 0.2 to 0.3 microns, and severe wear represents the specific wear greater than 0.3 microns. From the microstructural analysis of worn surface and debris, oxidation, softening and adhesion mechanisms were observed in the samples resulted with lower specific wear. Abrasion, adhesion and softening mechanisms were observed in the samples resulted with medium specific wear. Further, the wear mechanisms abrasion, softening, melting, and delamination were observed in the samples resulted with high specific wear.

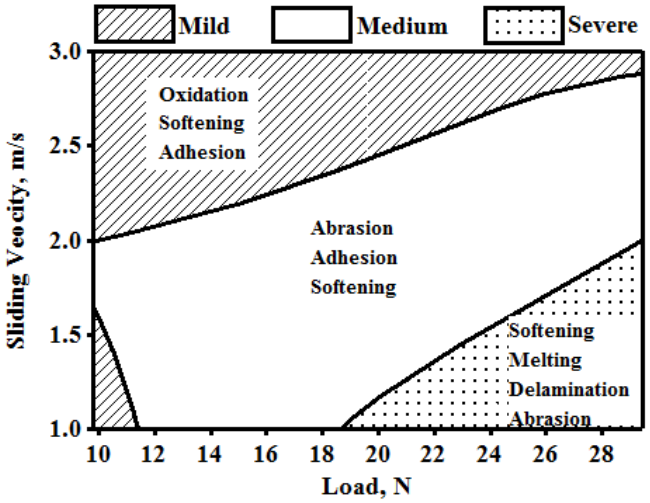

Figure 9: Wear map of (Mg-3Al)/5.6Ti metal-metal composite.

5.0 CONCLUSION

Magnesium based metal-metal composite (Mg-3Al)/5.6Ti was fabricated through the disintegrated melt deposition technique and examined metallurgically. Further, the dry sliding wear behaviour of the developed composite is investigated using pin-on-disc equipment. Following are the conclusions attained from the above research work.

The presence and dispersion of added metal elements in the magnesium metal-metal composite are studied by metallurgical analysis.

(a) Taguchi's approach and genetic algorithm technique yield the same optimal solution under the same optimum parameter to get minimum specific wear and coefficient of friction.

(b) A regression model was also developed and validated, by which specific wear and coefficient of friction were found to be predicted with the least percentage of error.

(c) Analysis of worn surfaces and collected debris, ascertained the occurrence of adhesion, delamination, softening and oxidation as the dominant wear mechanisms.

REFERENCES

Aydin, M., & Findik, F. (2010). Wear properties of magnesium matrix composites reinforced with SiO2 particles. Industrial Lubrication and Tribology, 62(4), 232–237.

Baskaran, S., Anandakrishnan, V., & Duraiselvam, M. (2014). Investigations on dry sliding wear behavior of in situ casted AA7075-TiC metal matrix composites by using Taguchi technique. Materials and Design, 60, 184–192.

Braszczyńska-Malik, K. N., & Przełożyńska, E. (2014). Metal-metal cast composites. Archives of Foundry Engineering, 14(3), 110–113.

Castro, M. M., Pereira, P. H. R., Isaac, A., Figueiredo, R. B., & Langdon, T. G. (2019). Development of a magnesium-alumina composite through cold consolidation of machining chips by high-pressure torsion. Journal of Alloys and Compounds, 780, 422-427.

Mehra, D., Mahapatra, M. M., & Harsha, S. P. (2018). Processing of RZ5-10wt% TiC in-situ magnesium matrix composite. Journal of magnesium and alloys, 6(1), 100-105.

Mehra, D., Mahapatra, M. M., & Harsha, S. P. (2018). Effect of wear parameters on dry abrasive wear of RZ5-TiC in situ composite. Industrial Lubrication and Tribology, 70(2), 256-263.

Elleuch, R., Elleuch, K., Mnif, R., Fridrici, V., Kapsa, P., & Khélifati, G. (2006). Comparative study on wear behaviour of magnesium and aluminium alloys. Proceedings of the Institution of Mechanical Engineers, Part J: Journal of Engineering Tribology, 220(6), 479–486.

Krishna, M. G., Kumar, K. P., Swapna, M. N., Rao, J. B., & Bhargava, N. R. M. R. (2017). Metal-metal Composites-An Innovative Way for Multiple Strengthening. Materials Today: Proceedings, 4(8), 8085–8095.

Habibi, M. K., Hamouda, A. S., & Gupta, M. (2013). Hybridizing boron carbide (B4C) particles with aluminum (Al) to enhance the mechanical response of magnesium based nano-composites. Journal of Alloys and Compounds, 550, 83–93.

Hassan, S. F., Ogunlakin, N. O., Al-Aqeeli, N., Nouari, S., Baig, M. M. A., & Patel, F. (2018). Development of tensile-compressive asymmetry free magnesium based composite using TiO2 nanoparticles dispersion. Journal of Materials Research, 33(2), 130–137.

Hou, J. T., Du, W. B., Wang, Z. H., Du, X., & Xu, C. (2018). Wet Powder Metallurgy Process for Dispersing Carbon Nanotubes and Fabricating Magnesium Composite. In Key Engineering Materials, 759, 86–91.

Maleque, M. A., Harina, L., Bello, K., Azwan, M., & Rahman, M. M. (2018). Tribological properties of surface modified Ti-6Al-4V alloy under lubricated condition using Taguchi approach. Jurnal Tribologi, 17, 15-28.

Metawa, N., Hassan, M. K., & Elhoseny, M. (2017). Genetic algorithm based model for optimizing bank lending decisions. Expert Systems with Applications, 80, 75–82.

Monikandan, V. V., Joseph, M. A., & Rajendrakumar, P. K. (2018). Application of full factorial design to study the tribological properties of AA6061-B4C and AA6061-B4C-MoS2 composites. Jurnal Tribologi, 16, 31-32.

Mukhopadhyay, A., Duari, S., Barman, T. K., & Sahoo, P. (2016). Optimization of Wear Behavior of Electroless Ni-P-W Coating under Dry and Lubricated Conditions Using Genetic Algorithm (GA). Jurnal Tribologi, 11, 24–48.

Niranjan, C. A., Srinivas, S., & Ramachandra, M. (2018). Effect of process parameters on depth of penetration and topography of AZ91 magnesium alloy in abrasive water jet cutting. Journal of Magnesium and Alloys, 6(4), 366–374.

Rashad, M., Pan, F., Asif, M., She, J., & Ullah, A. (2015). Improved mechanical proprieties of "magnesium based composites" with titanium-aluminum hybrids. Journal of Magneisum and Alloys, 3(1), 1–9.

Sankaranarayanan, S., Jayalakshmi, S., & Gupta, M. (2011). Effect of addition of mutually soluble and insoluble metallic elements on the microstructure, tensile and compressive properties of pure magnesium. Materials Science and Engineering: A, 530, 149–160.

Saravanan, C., Subramanian, K. Anandakrishnan, V., & Sathish, S. (2018). Tribological behavior of AA7075-TiC composites by powder metallurgy. Industrial Lubrication and Tribology, 70(6), 1066–1071.

Sarkar, S., Baranwal, R. K., Lamichaney, S., De, J., & Majumdar, G. (2018). Optimization of electroless Ni-Co-P coating with hardness as response parameter : A computational approach. Jurnal Tribologi, 18, 81–96.

Sathish, S., Anandakrishnan, V., & Gupta, M., (2019). Optimization of Tribological Behavior of Magnesium Metal-Metal Composite Using Pattern Search and Simulated Annealing Techniques. Materials Today: Proceedings. https://doi.org/10.1016/j.matpr.2019.06.643

Selvam, B., Marimuthu, P., Narayanasamy, R., Anandakrishnan, V., Tun, K. S., Gupta, M., & Kamaraj, M. (2014). Dry sliding wear behaviour of zinc oxide reinforced magnesium matrix nano-composites. Materials and Design, 58, 475–481.

Turan, M. E., Sun, Y., & Akgul, Y. (2018a). Improved wear properties of magnesium matrix composite with the addition of fullerene using semi powder metallurgy. Fullerenes, Nanotubes and Carbon Nanostructures, 26(2), 130–136.

Turan, M. E., Sun, Y., & Akgul, Y. (2018b). Mechanical, tribological and corrosion properties of fullerene reinforced magnesium matrix composites fabricated by semi powder metallurgy. Journal of Alloys and Compounds, 740, 1149–1158.

Kaviti, R. V. P., Jeyasimman, D., Parande, G., Gupta, M., & Narayanasamy, R. (2018). Investigation on dry sliding wear behavior of Mg/BN nanocomposites. Journal of Magneisum and Alloys, 6(3), 263–276.

Wang, M., Zhao, Y., Wang, L. D., Zhu, Y. P., Wang, X. J., Sheng, J., Yang, Z., Shi, H., & Fei, W. D. (2018). Achieving high strength and ductility in graphene/magnesium composite via an in-situ reaction wetting process. Carbon, 139, 954–963.

Watanabe, H., Ikeo, N., & Mukai, T. (2018). Processing and Mechanical Properties of a Tricalcium Phosphate-Dispersed Magnesium-Based Composite. Materials Transactions, 60(1), 105–110.

Yu, W., Zhao, H., Wang, X., Wang, L., Xiong, S., Huang, Z., Li, S., Zhou, Y., & Zhai, H. (2018). Synthesis and characterization of textured Ti2AlC reinforced magnesium composite. Journal of Alloys and Compounds, 730, 191–195.

Zain, A. M., Haron, H., & Sharif, S. (2011). Genetic Algorithm and Simulated Annealing to estimate optimal process parameters of the abrasive waterjet machining. Engineering with Computers, 27(3), 251–259.

Zhang, L., Luo, X., Liu, J., Leng, Y., & An, L. (2018). Dry sliding wear behavior of Mg-SiC nanocomposites with high volume fractions of reinforcement. Materials Letters, 228, 112–115.

Zhang, L., Wang, Q., Liu, G., Guo, W., Ye, B., Li, W., Jiang, H., & Ding, W. (2018). Tribological Behavior of Carbon Nanotube-Reinforced AZ91D Composites Processed by Cyclic Extrusion and Compression. Tribology Letters, 66(2), 66–71.